



Mechanical characterization of lightweight foam-based sandwich panels

Cristina Vălean^{a,b,*}, Corina Șoșdean^{c,*}, Liviu Marșavina^a, Emanoil Linul^{a,*}

^a Department of Mechanics and Strength of Materials, Politehnica University of Timisoara, M. Viteazu Blvd., No. 1, Timisoara 300 222, Romania

^b Research Institute for Renewable Energies, Politehnica University of Timisoara, Musicescu Gavril Str., No. 138, Timisoara 300 774, Romania

^c Department of Mechatronics, Politehnica University of Timisoara, M. Viteazu Blvd., No. 1, Timisoara 300 222, Romania

ARTICLE INFO

Article history:

Received 15 October 2020

Received in revised form 24 November 2020

Accepted 1 December 2020

Available online 21 January 2021

Keywords:

Rigid polyurethane foam

Foam-based sandwich panels

Experimental tests

Mechanical properties

ABSTRACT

Foam-based composite structures are widely used in the field of construction market for roofing and closing walls. This paper presents a mechanical characterization of a lightweight sandwich panels with foam core. The faces of the panels are made of thin steel sheets, and for the core, closed-cell polyurethane foam with a density of 40 kg/m³ was used. Mechanical testing consists of quasi-static four-point bending, transversal tensile and compression tests. All experimental tests were conducted at room temperature in accordance to EN 14509:2013 Standard. With the data obtained from experimental tests, load–displacement curves and mechanical properties are presented. Following the experimental tests, the elastic characteristics (shear modulus, tensile E-modulus, compression modulus), strength properties (ultimate shear strength, transverse tensile strength, compression strength) and energy absorption performances were determined.

© 2021 Elsevier Ltd. All rights reserved.

Selection and peer-review under responsibility of the scientific committee of the 8th International Conference on Advanced Materials and Structures - AMS 2020.

1. Introduction

In recent years, due to their special characteristics, foams have become attractive for various top industries and household applications [1–3]. The most important attributes of foam materials are high capacity to absorb impact energy and high strength per unit weight. Other advantages are good thermal insulation property and variable density when compared to solid materials [4–6]. Moreover, the polymeric foams are commonly used in structural engineering applications due to the weight saving and stiffening performances they can offer in the design process (e.g., sandwich cores) [7–9]. Therefore, foam-based composite structures are of major interest especially in the field of lightweight construction. They can be easily produced in numerous structural forms by a comprehensive variety of manufacturing methods using chemical or physical blowing agents [10–12].

Over the years, many experimental, analytical and numerical investigations have been carried out on polymeric foams and

reinforced polymeric foams, while limited studies are conducted on real sandwich structures. Linul et al. [13–15] investigated the influence of density, temperature, loading speed and anisotropy on the compressive mechanical behaviour of rigid polyurethane (PUR) foams. They found that the density and test temperature significantly influence the main properties of the PUR foams, while the loading speed and foam anisotropy do not show major differences [13]. Moreover, the authors determined the optimal density of the PUR foam (in the range of 40–300 kg/m³), using efficiency diagrams and energy absorption methods [14]. Moreover, waste tire particles [16] short glass-fibres, glass micro-spheres and chopped glass-fibre strands [17] aluminium microfibers [18] coffee grounds [19] potato protein [20] buffing dust [21] cellulose nanocrystals [22] wheat straw lignin [23] have been used to improve the mechanical properties of the sandwich core materials. Researchers found that compared to neat foam, the reinforced foams were characterized by superior dimensional stability and higher mechanical/physical/thermal properties. Linul and Marsavina [24] studied the three point bending behaviour of five different sandwich beams. Depending on the type of faces (material and thickness) and core density (40 and 200 kg/m³), the authors obtained different collapse mechanisms (face yield and face wrinkling). Based on the experimentally determined properties, they created the characteristic failure-mode maps. The various failure

* Corresponding authors at: Department of Mechanics and Strength of Materials, Politehnica University of Timisoara, M. Viteazu Blvd., No. 1, Timisoara 300 222, Romania (C. Vălean).

E-mail addresses: cristina_valean@yahoo.com (C. Vălean), corina.sosdean@yahoo.com (C. Șoșdean), emanoil.linul@upt.ro (E. Linul).

modes of sandwich beams were studied by Daniel and Gdoutos [25]. They varied certain parameters (e.g. beam dimensions, loading or state of stress) and identified the transition from one failure mode to another. In addition, the authors compared analytical predictions with experimental results. In order to reveal the operative collapse mode as a function of geometry of sandwich beam with PVC foam core subjected to three point bending, Steeves and Fleck [26,27] developed different failure mechanism maps. They observed that the analytic expressions become inappropriate and the analytic models are inaccurate for sandwich beams with thick faces relative to the core thickness [27].

Most studies have focused on the individual characterization of the sandwich core (compression tests), or the creation of sandwich beams failure-mode maps (three-point bending tests). Therefore, this paper aims at a complete characterization of a foam-based sandwich panel by performing four-point bending, tensile and compression tests. The obtained mechanical characteristics can be used for the analytical determination of the capable load of large sandwich structures.

2. Materials and methods

2.1. Materials and sample preparation

Double skin metal faced insulating panels with a polyurethane foam core were chosen in order to determine the main mechanical properties. The panels faces are made of steel with a modulus of elasticity of $E = 2.1 \cdot 10^5$ MPa, while the core has a density of 40 kg/m^3 . The density of the core material was determined by dividing the mass of the sample by its volume.

For the complete mechanical characterization of the foam-based composite structure, bending, tensile and compression samples were prepared. All samples were obtained according to EN 14509:2013 Standard [28] from a large sandwich panel with lightly profiled faces. The samples were taken from a range of positions covering the width of the composite panel. Fig. 1 shows the geometrical parameters of the bending sample, as well as the dimensions and positioning of the metal load spreading plates.

According to EN 14509:2013 Standard [28] tensile and compression samples shall be of square cross-section having side dimensions between 100 mm and 300 mm. Therefore, the tensile and compression samples presented a prismatic shape with the dimensions 120 mm (height) \times 100 mm (width) \times 100 mm (thickness), and 70 mm (height) \times 100 mm (width) \times 100 mm (thickness), respectively. Fig. 2 shows a manufactured sample from each mentioned category, together with their fixing in the loading devices of the used testing machine.

2.2. Experimental program

The experimental evaluation of the sandwich panel consisted in performing several types of quasi-static tests, namely: four-point bending, transverse tensile and compression tests. The four-point bending (Fig. 2a) and transverse tensile (Fig. 2b) tests were carried out using a Zwick/Roell Z005 testing machine with a load-cell capacity of 5 kN, equipped with a Test Xpert II v1.43 software. Due to the large dimensions of the samples imposed by the EN 14509:2013 standard [28] and also the need to develop a higher force, the compression tests (Fig. 2c) were performed on the LBG TC100 universal test machine. The machine is equipped with a load-cell capacity of 100 kN, respectively with a TC Soft 2004 Plus software specialized in data processing.

All the experimental tests were performed at room temperature, under normal humidity conditions, with a loading velocity of 10 mm/min. The tests followed the EN 14509:2013 standard [28] instructions.

3. Results and discussions

Following the four-point bending, tensile and compression tests, the force–displacement curves were obtained. Fig. 3a shows the most representative curve resulting from the four-point bending tests. The curve shows a narrow area of sample settlement in the test device, followed by an extended linear-elastic area [29,30]. The linear-elastic zone is followed by a yield of the sandwich structure faces, and finally by the shearing of the core. The failure occurs suddenly with a core shear at an angle of about 45 degrees (Fig. 3b). The shear band is located between the upper-right loading point and the lower-right support point. From Fig. 3a it can be observed that the core shear occurred at a displacement of 11.12 mm.

Based on the results obtained from the four-point bending tests and the geometrical parameters of the samples, the ultimate shear strength f_{cv} was calculated using equation (1):

$$f_{cv} = k_v \frac{F_u}{2Be} \quad (1)$$

where F_u is the ultimate load carried by the sample failing in shear, k_v is the reduction factor for cut ends in pre-formed cores, B is the width of the sample and e is the depth between the centroids of the sandwich faces. Because the investigated sandwich panel was formed in-situ, in this case the k_v factor was considered equal to 1.

In addition, the shear modulus of the core material, G_c , was calculated from the slope of the straight part of the load–displacement curve, using the Equation (2):

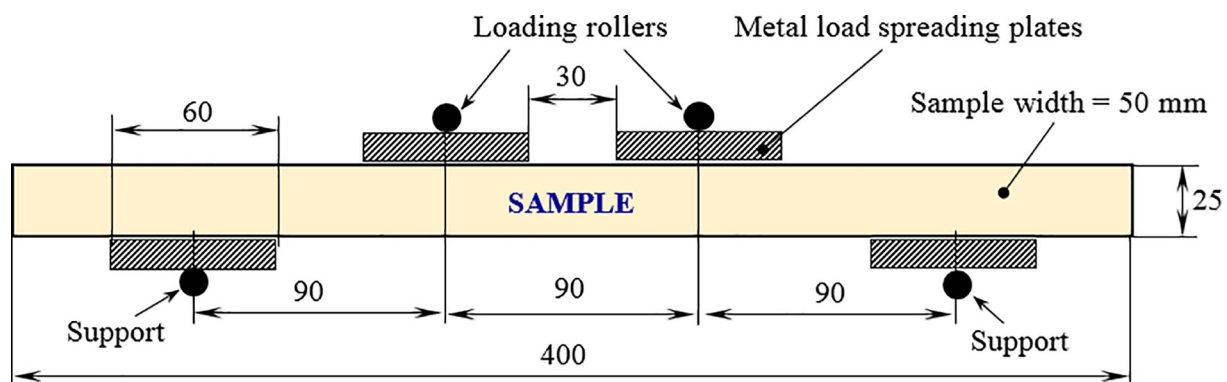


Fig. 1. Dimensions of the bending sample and positioning of the metal load plates, in mm.

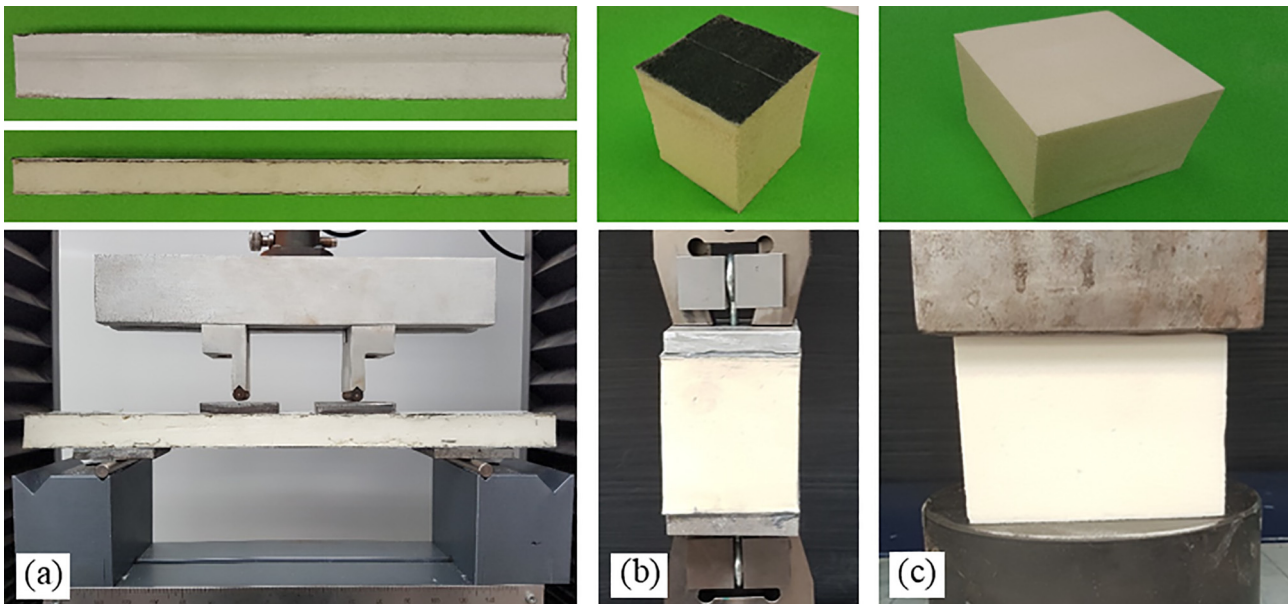


Fig. 2. Obtained samples (top) together with their fixing in the loading devices of the used testing machine (bottom).

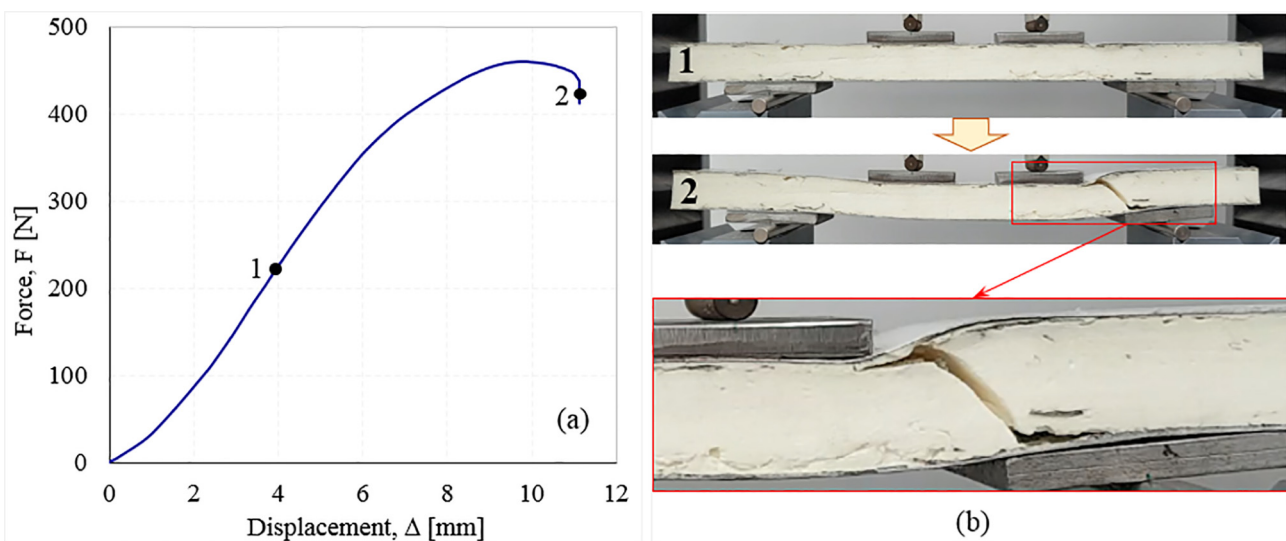


Fig. 3. (a) Four-point bending force–displacement curve; (b) deformation sequences of the sample during four-point bending test.

$$G_c = \frac{\Delta FL}{6Bd_c \Delta w_s} \quad (2)$$

where L is the span of test sample at shear failure, d_c is the thickness of the core material, Δw_s is the shear deflection and is calculated with equation (3):

$$\Delta w_s = \Delta w - \Delta w_B \quad (3)$$

where Δw is the deflection at mid-span for a load increment ΔF taken from the slope of the linear-elastic part of the load–displacement curve and Δw_B is the bending deflection calculated as follows:

$$\Delta w_B = \frac{\Delta FL^3}{56,34B_S} \quad (4)$$

with B_S as the flexural rigidity, which is determined with Equation (5):

$$B_S = \frac{E_{F1} \cdot A_{F1} \cdot E_{F2} \cdot A_{F2}}{E_{F1} \cdot A_{F1} + E_{F2} \cdot A_{F2}} e^2 \quad (5)$$

where E_{F1} and E_{F2} are the E-modulus of the top and bottom faces, while A_{F1} and A_{F2} are the cross-section areas of the top and bottom sandwich faces.

Therefore, by using Equation (1), an average value of 0.227 MPa for the ultimate shear strength f_{cv} was obtained. Moreover, by replacing the data from Equations (3)–(5) in Equation (2), a value of 4.298 MPa was determined for shear modulus of the core material G_c .

The tensile force–displacement curve is shown in Fig. 4a. Both on the graph (Fig. 4a) and on the broken sample (Fig. 4b) it can be seen that the investigated sandwich panel highlights a brittle behaviour under tensile loads [31,32]. The failure of the sample occurs in the upper part of the core and not in adhesive, this validating the test.

Dividing the ultimate tensile load by the cross-sectional area (A) of the sample, the maximum transverse tensile strength ($f_{ct, max}$) of the sandwich panel can be calculated. After replacing the data, an $f_{ct, max}$ value of 0.160 MPa was obtained. In addition, the deforma-

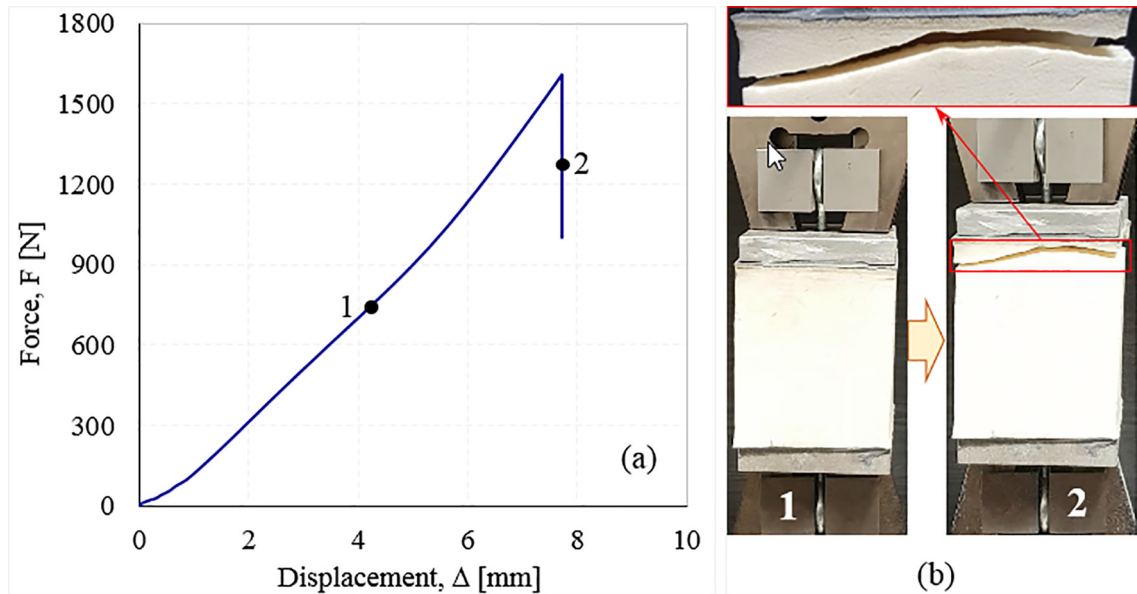


Fig. 4. (a) Tensile force–displacement curve; (b) deformation sequences of the sample during transverse tensile test.

tion corresponding to the tensile strength ($\Delta f_{Ct, \max}$) was found around 6.487%.

Furthermore, in order to determine the tensile E-modulus of the core (E_{Ct}), the Equation (6) was used:

$$E_{Ct} = \frac{F_u d_c}{w_u A} \quad (6)$$

where d_c is the sample thickness and w_u is the ideal displacement at tensile ultimate load based on the linear-elastic part of the load–displacement curve. Thus, the E had an average value of 2.265 MPa.

Regarding the compression behaviour (Fig. 5a), it can be seen that the force–displacement curve is totally different from the other two previously obtained (Fig. 3a and 4a). In this case, the curve shows three characteristic areas typical of cellular materials [33–35]. Initially, a very short linear-elastic area is identified that ends with the yield of the material. From this area the compressive modulus (E), the yield stress (σ_y), respectively the deformation (ϵ_y) corresponding to the σ_y are determined. Beyond this area is a long plateau area, which highlights a permanent hardening. Characteristic of this area is the plateau stress (σ_{pl}), which is determined as

an average of the stresses corresponding to 20% ($\sigma_{20\%}$) and 40% ($\sigma_{40\%}$) strain, respectively. Finally, the curve ends with the densification area, where the specimen compaction takes place. This area begins with the onset strain of densification (ϵ_d), corresponding to the densification stress (σ_d). The σ_d represents 1.3 of the σ_{pl} . Characteristic of plateau-densification areas is also the energy absorption capacity (W_d), represented by the area under the curve. This was determined using the Equation (7) [36–38].

$$W_d = \int_0^{\epsilon} \sigma d\epsilon \quad (7)$$

The PUR foam showed a compressive modulus of 1.59 MPa. The values of strength properties (σ_y , σ_{pl} and σ_d) and energy absorption performances (W_d) are shown in Fig. 6. The main value obtained for densification strain was 42.19%.

In the design calculations of buildings, halls, etc., it is necessary to know in advance their strength. Of course, the mechanical properties of sandwich structures are determined in laboratory conditions, on standardized samples. However, using the properties determined on standardized samples and imposing various

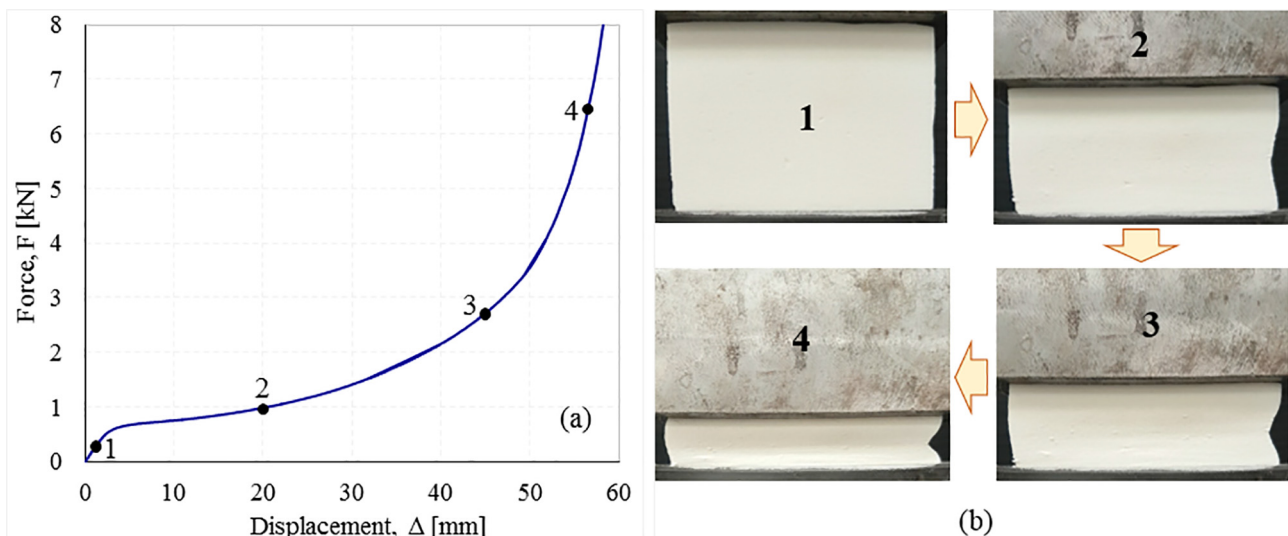


Fig. 5. (a) Compression force–displacement curve; (b) deformation sequences of the sample during compression test.

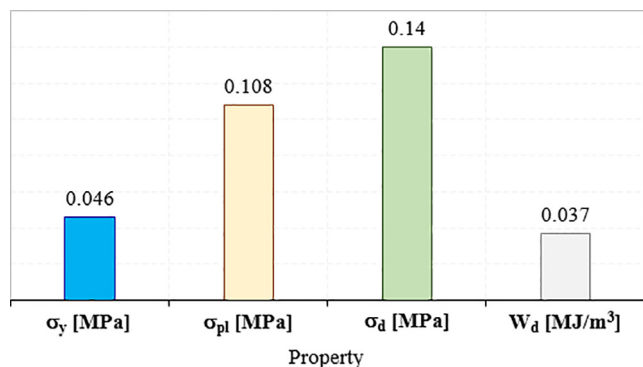


Fig. 6. Strength and energy absorption properties of PUR foam core.

conditions (face yield, core shear and strength condition), capable load calculations can be made on sandwich panels with dimensions that far exceed the values of those tested in the laboratory.

4. Conclusions

This paper investigates the mechanical behaviour of foam-based sandwich panel at different quasi-static loads. For this purpose, four-point bending, tensile and compression tests were performed on both the sandwich panels (bending and tensile tests) and the core material (compression tests). Steel sheets were used as sandwich faces, while a polyurethane foam with a density of 40 kg/m³ represented the sandwich core. The following conclusions can be drawn:

- Following the four-point bending tests, a core shear of the sandwich panel was obtained. A value of 0.227 MPa for the ultimate shear strength and 4.298 MPa for shear modulus of the core material were obtained.
- In transverse tensile test, the foam-based composite structure showed a brittle behaviour until final failure, the fracture taking place in the core and not at the core-face interface. No plastic deformations were observed on the tested specimens. In this case, the maximum transverse tensile strength and tensile E-modulus of the core had the values of 0.160 and 2.265 MPa, respectively.
- The compressive force–displacement curves highlighted three distinct areas, as follows: linear-elastic, plateau and densification. Values of 0.046 MPa for compression strength and 1.59 MPa for compression modulus were obtained. In addition, the energy absorption performances were around of 0.037 MJ/m³, while the densification strain was 42.19%.
- The obtained mechanical properties can be used in the analytical calculations of sandwich panels for capable loads.

CRedit authorship contribution statement

Cristina Vălean: Conceptualization, Investigation, Writing - original draft, Writing - review & editing. **Corina Şoşdean:** Formal analysis, Investigation, Writing - original draft, Writing - review & editing. **Liviu Marşavina:** Conceptualization, Methodology, Formal analysis, Resources, Software, Writing - original draft, Writing - review & editing, Supervision. **Emanoil Linul:** Conceptualization, Methodology, Investigation, Resources, Writing - original draft, Writing - review & editing.

Declaration of Competing Interest

The authors declare that they have no known competing financial interests or personal relationships that could have appeared to influence the work reported in this paper.

Acknowledgements

This work was partially supported by research project of the Romanian Ministry of Research and Innovation, CCCDI – UEFISCDI, project number PN-III-P1-1.2-PCCDI-2017-0391 / CIA_CLIM - Smart buildings adaptable to the climate change effects, within PNCDI III”.

References

- [1] L.J. Gibson, M.F. Ashby, Cellular Solids-Structures and properties-Second edition, Published by the Press Syndicate of the University of Cambridge, UK, 1997.
- [2] A. Farshidi, C. Berggreen, L.A. Carlsson, J. Sandw. Struct. Mater. (2018).
- [3] E. Linul, L. Marşavina, C. Vălean, R. Bănică, Eng. Fract. Mech. 225 (2020) 106274.
- [4] M.S. Thompson, I.D. McCarthy, L. Lidgren, L. Ryd, J. Biomech. Eng. 125 (5) (2003) 732–734.
- [5] N.J. Mills, Polymer Foams Handbook, Butterworth-Heinemann, 2007.
- [6] L. Marsavina, A. Cernescu, E. Linul, et al., Materiale Plastice 47 (1) (2010) 85–89.
- [7] H. Abbasi, M. Antunes, J.I. Velasco, Polymers 10 (2018) 348.
- [8] D.K. Rajak, D.D. Pagar, P.L. Menezes, et al., Polymers 11 (10) (2019) 1667.
- [9] L. Marsavina, E. Linul, Fatig. Fract. Eng. Mater. Struct. 43 (11) (2020) 2483–2514.
- [10] Y. Sun, B. Amirrasouli, S.B. Razavi, et al., Acta Mater. 110 (2016) 161–174.
- [11] M.R.M. Aliha, S.S. Mousavi, A. Bahmani, et al., Theor. Appl. Fract. Mech. 101 (2019) 152–161.
- [12] M.F. Ashby, A. Evans, N.A. Fleck, et al., Metal Foams: A Design Guide, Butterworth-Heinemann, USA, 2000.
- [13] E. Linul, T. Voiconi, L. Marsavina, T. Sadowski, J. Phys. Conf. Ser. 451 (2013) 012002.
- [14] E. Linul, D.A. Şerban, L. Marsavina, T. Sadowski, Arch. Civ. Mech. Eng. 17 (3) (2017) 457–466.
- [15] E. Linul, D.A. Şerban, T. Voiconi, et al., Key Eng. Mater. 601 (2014) 246–249.
- [16] G. Soto, A. Castro, N. Vecchiatti, et al., Polym. Test. 57 (2017) 42–51.
- [17] S.K. Khanna, S. Gopalan, Reinforced polyurethane flexible foams. In Compliant Structures in Nature and Engineering, WIT Press: Billerica, MA, USA, 2005.
- [18] E. Linul, C. Vălean, P.A. Linul, Polymers 10 (12) (2018) 1298.
- [19] N. Gama, R. Silva, A.P.O. Carvalho, et al., Polym. Test. 62 (2017) 13–22.
- [20] S. Członka, M.F. Bertino, K. Strzelec, Polym. Test. 68 (2018) 135–145.
- [21] S. Członka, M.F. Bertino, K. Strzelec, et al., Polym. Test. 69 (2018) 225–237.
- [22] X. Zhou, M.M. Sain, K. Oksman, Compos. Part A Appl. Sci. Manuf. 83 (2016) 56–62.
- [23] A. Paberza, U. Cabulis, A. Arshanitsa, Polimery/Polymers 59 (2014) 477–481.
- [24] E. Linul, L. Marsavina, Proc. Romanian Acad. – Ser. A 16 (4) (2015) 522–530.
- [25] I.M. Daniel, E.E. Gdoutos, K.A. Wang, et al., Int. J. Dam. Mech. 11 (2002) 309–334.
- [26] C.A. Steeves, N.A. Fleck, Int. J. Mech. Sci. 46 (2004) 461–583.
- [27] C.A. Steeves, N.A. Fleck, Int. J. Mech. Sci. 46 (2004) 585–608.
- [28] EN 14509:2013, Self-supporting double skin metal faced insulating panels - Factory made products - Specifications, 2013.
- [29] T. Voiconi, E. Linul, L. Marsavina, et al., Solid State Phenom. 216 (2014) 116–121.
- [30] M. Antunes, J.I. Velasco, Prog. Polym. Sci. 39 (2014) 486–509.
- [31] S.N.I. Kudori, H. Ismail, S.R. Khimi, Mater. Today: Proc. 17 (2019) 609–615.
- [32] L. Marsavina, D.M. Constantinescu, E. Linul, et al., Eng. Fract. Mech. 167 (2016) 68–83.
- [33] O. Khezrzadeh, O. Mirzaee, E. Emadoddin, et al., Materials 13 (10) (2020) 2329.
- [34] B. Katona, A. Szlancsik, T. Tábi, I.N. Orbulov, Mat. Sci. Eng. A-Struct. 739 (2019) 140–148.
- [35] D.K. Rajak, N.N. Mahajan, E. Linul, J. Alloys Compd. 775 (2019) 675–689.
- [36] I.N. Orbulov, A. Szlancsik, A. Kemény, D. Kincses, Compos. Part A Appl. Sci. Manuf. 135 (2020) 105923.
- [37] D. Pietras, E. Linul, T. Sadowski, A. Rusinek, Compos. Struct. 249 (2020) 112548.
- [38] G. Epasto, F. Distefano, L. Gu, et al., Mater. Design 196 (2020) 109120.